Successive Slepian Subspace Projection in Time and Frequency for Time-Variant Channel Estimation

Thomas Zemen, Helmut Hofstetter
Forschungszentrum Telekommunikation Wien
Donau-City-Strasse 1
1220 Vienna, Austria.
E-mail: {thomas.zemen, hofstetter}@ftw.com

Gerhard Steinböck
ARC Seibersdorf research GmbH.
Donau-City-Strasse 1
1220 Wien, Austria.
Email: Gerhard.Steinboeck@arcs.ac.at

***Abstract*— This paper describes an iterative time-variant channel estimator for the uplink of a multi-carrier code division multiple access (MC-CDMA) system. MC-CDMA is based on orthogonal frequency division multiplexing (OFDM). Due to OFDM every time-variant frequency-flat subcarrier can be estimated individually. We develop a successive Slepian subspace projection in the time and frequency domain. The subspace in the time domain is spanned by discrete prolate spheroidal (DPS) sequences. The DPS sequences are designed according to two system parameters, the maximum Doppler bandwidth and the block length. The correlation between the individual subcarriers can be exploited by a subspace projection in the frequency domain, using so called shifted DPS sequences. The shifted DPS sequences are designed according to the maximum essential support of the channel impulse response and the number of subcarriers. Due to the subspace projection in the frequency domain the presented channel estimator is able to deal with realistic channels that have non sample-spaced path delays. We validate the channel estimator with a geometry based stochastic channel model according to the COST 259 recommendations.**

I. Introduction

For time-variant channel modeling it is common to assume a delay-tap line with sample-spaced (discrete) path delays. However, realistic channels have real-valued path delays. In this paper we develop an iterative time-variant channel estimator that is *not* limited by the assumption of sample-spaced (discrete) path delays. We show the application of this time-variant channel estimator in a multi-user multi-carrier code division multiple access (MC-CDMA) uplink scenario [1]. MC-CDMA is based on orthogonal frequency division multiplexing (OFDM) utilizing a user specific random spreading sequence in the frequency domain.

The variation of a wireless channel over the duration of a data block is caused by user mobility and multipath propagation. The Doppler shifts on the individual paths depend on the user's velocity v, the carrier frequency f_{C}, and the scattering environment. The maximum variation in time of the wireless channel is upper bounded by the maximum (one sided) normalized Doppler bandwidth $\nu_{\mathrm{Dmax}} = B_{\mathrm{D}} T_{\mathrm{S}}$ where the maximum Doppler bandwidth $B_{\mathrm{D}} = v_{\max} f_{\mathrm{C}} / c_0$, $v_{\max}$ is the maximum (supported) velocity, T_{S} is the symbol duration, and c_0 denotes the speed of light.

We apply OFDM in order to transform the time-variant frequency-selective channel into a set of parallel time-variant frequency-flat subcarriers. The sequence of channel coefficients for every time-variant frequency-flat subcarrier is bandlimited by ν_{Dmax}. It was shown by Slepian [2], that time-limited parts of bandlimited sequences span a low-dimensional subspace. A natural set of basis functions for this subspace is given by the so-called discrete prolate spheroidal (DPS) sequences. A Slepian basis expansion using this subspace representation was proposed in [3] for time-variant channel equalization. It was shown in [4] that the channel estimation bias obtained with the Slepian basis expansion is more than a magnitude smaller compared to the Fourier basis expansion (i.e. a truncated discrete Fourier transform) [5].

The Slepian basis expansion coefficients are estimated individually for every subcarrier. These channel estimates can be further improved by exploiting the correlation between the individual subcarriers. For this purpose a truncated Fourier transform was used in [6] for a sample-spaced delay tap-line model.

For more realistic non-sample-spaced delay tap-line models [7] Edfors et al. [8] exploited the correlation in the frequency domain by using the singular value decomposition of the channels covariance matrix which is assumed to be known. In [9] the singular value decomposition was calculated in an adaptive manner using an estimate of the covariance matrix.

Contributions:

- In this paper we show that frequency shifted DPS sequences span the natural subspace for noise suppression for non-sample-spaced delay tap-line channels and provide an analytic error expression.
- We develop a channel estimator that does not require detailed knowledge about the autocorrelation and the power delay profile of the channel. Only a maximum velocity of the mobile station and a maximum essential support of the impulse response needs to be assumed.
- We validate the time-variant channel estimator using a geometry based stochastic channel model (GSCM) according to the COST 259 recommendations.

This work was carried out with funding from K*plus* in the ftw. projects I0 'Signal and Information Information Processing' and C9 'MIMO-UMTS for future packet services' together with Infineon Technologies and ARC Seibersdorf research GmbH.

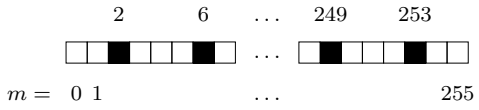

Fig. 1. Pilot pattern defined by (1) for block length $M = 256$ and $J = 60$ pilot symbols.

Section II briefly discusses the receive algorithm and introduces the signal model. The time-variant channel estimator using a Slepian subspace projection in the time domain is reviewed in Section III. The frequency domain Slepian subspace projection is explained in Section IV and an analytic error expression is derived in Section V. Section VI gives a short introduction into the GSCM. We provide the system parameters in Section VII and validate our channel estimator with the GSCM channel model in Section VIII. Conclusions are drawn in Section IX.

II. Signal Model for Time and Frequency Selective Channels.

We consider the equalization and detection problem for a K user MC-CDMA uplink. Each user's data symbols are spread over N subcarriers by means of a user-specific spreading code. The transmission is block-oriented with block length M; a data block consists of $M - J$ OFDM data symbols and J OFDM pilot symbols.

The data symbols $b_k[m]$ result from the binary information sequence $\chi_k[m'']$ of length $2(M - J)R_C$ by convolutional encoding with code rate R_C, random interleaving and quadrature phase shift keying (QPSK) modulation with Gray labelling. The data symbols are given by $b_k[m] \in \{\pm 1 \pm \mathrm{j}\}/\sqrt{2}$ for $m \notin \mathcal{P}$ and $b_k[m] = 0$ for $m \in \mathcal{P}$, where the pilot placement is defined by the index set

$$\mathcal{P} = \{\lfloor M/J(i + 1/2) \rfloor \mid i = 0, \ldots, J - 1\} \tag{1}$$

and discrete time at rate $1/T_\mathrm{S}$ is denoted by m, see Fig. 1. Each symbol is spread by a random spreading sequence $\boldsymbol{s}_k \in \mathbb{C}^N$ with independent identically distributed (i.i.d.) elements chosen from the set $\{\pm 1 \pm \mathrm{j}\}/\sqrt{2N}$. After the spreading operation, pilot symbols $\boldsymbol{p}_k[m] \in \mathbb{C}^N$ with elements $p_k[m, e]$ are added, giving the $N \times 1$ vectors

$$\boldsymbol{d}_k[m] = \boldsymbol{s}_k b_k[m] + \boldsymbol{p}_k[m]\,. \tag{2}$$

The elements of the pilot symbols $p_k[m, e]$ for $m \in \mathcal{P}$ and $e \in \{0, \ldots, N - 1\}$ are randomly chosen from the QPSK symbol set $\{\pm 1 \pm \mathrm{j}\}/\sqrt{2N}$. For $m \notin \mathcal{P}$ we define $\boldsymbol{p}_k[m] = \boldsymbol{0}_N$. Subsequently, an N-point inverse discrete Fourier transform (DFT) is carried out and a cyclic prefix of length G is inserted. An OFDM symbol, including the cyclic prefix, has length $P = N + G$ chips. The chip rate $1/T_\mathrm{C} = P/T_\mathrm{S}$.

We describe the time-variant impulse response $h(t, \tau)$ as the superposition of R individual paths

$$h(t, \tau) = \sum_{r=1}^{R} \alpha_r(t)\delta(t - \tau_r(t)). \tag{3}$$

Each path is characterized by its time-variant attenuation $\alpha_r(t) = \alpha'_r \mathrm{e}^{2\pi f_r t}$ and its *real-valued* time-variant delay $\tau_r(t)$. These parameters are modelled with a GSCM which is described in more detail in Section VI.

Under the assumption of small inter-carrier interference [10] we are able to represent the time-variant channel for the processing at the receive side by the frequency response vector $\boldsymbol{g}_k[m] \in \mathbb{C}^N$. The received signal after cyclic prefix removal and DFT is

$$\boldsymbol{y}[m] = \sum_{k=1}^{K} \mathrm{diag}(\boldsymbol{g}_k[m])\boldsymbol{d}_k[m] + \boldsymbol{v}[m] \tag{4}$$

where complex additive white Gaussian noise with zero mean and covariance $\sigma_v^2 \boldsymbol{I}_N$ is denoted by $\boldsymbol{v}[m] \in \mathbb{C}^N$ with elements $v[m, e]$. We define the time-variant effective spreading sequences

$$\tilde{\boldsymbol{s}}_k[m] = \mathrm{diag}\left(\boldsymbol{g}_k[m]\right) \boldsymbol{s}_k\,, \tag{5}$$

and the time-variant effective spreading matrix $\tilde{\boldsymbol{S}}[m] = [\tilde{\boldsymbol{s}}_1[m], \ldots, \tilde{\boldsymbol{s}}_K[m]] \in \mathbb{C}^{N \times K}$. Using these definitions, we write the signal model for data detection as

$$\boldsymbol{y}[m] = \tilde{\boldsymbol{S}}[m]\boldsymbol{b}[m] + \boldsymbol{v}[m] \quad \text{for} \quad m \notin \mathcal{P} \tag{6}$$

where $\boldsymbol{b}[m] = [b_1[m], \ldots, b_K[m]]^\mathrm{T} \in \mathbb{C}^K$ contains the stacked data symbols for K users. We apply iterative parallel interference cancelation (PIC) and minimum mean square error (MMSE) filtering as described in [11], [12]. The output of the MMSE filter is used as input to the BCJR decoder after de-mapping and deinterleaving.

III. Slepian Subspace Projection in the Time Domain

The performance of the iterative receiver crucially depends on the estimation accuracy of the time-variant frequency response estimate $\boldsymbol{g}_k[m]$ since the effective spreading sequence (5) directly depends on the actual channel realizations. The signal model (4) describes a transmission over N parallel frequency-flat channels. Therefore, we rewrite (4) as a set of equations for every subcarrier $e \in \{0, \ldots, N - 1\}$,

$$y[m, e] = \sum_{k=1}^{K} g_k[m, e]d_k[m, e] + v[m, e]\,, \tag{7}$$

where $d_k[m, e] = s_k[e]b_k[m] + p_k[m, e]$.

The temporal variation of each subcarrier coefficient $g_k[m, e]$ is bandlimited by the normalized maximum Doppler bandwidth ν_Dmax. The normalized Doppler shifts $\nu_r = f_r T_\mathrm{S}$ of each path r fulfill $\nu_r \leq \nu_\mathrm{Dmax}$. We estimate $g_k[m, e]$ for an interval with block length M using the received sequence $y[m, e]$. We describe the time variation of $g_k[m, e]$ in (7) through the Slepian basis expansion [4], [3]

$$g_k[m, e] \approx \tilde{g}_k[m, e] = \sum_{i=0}^{D-1} u_i[m]\psi_k[i, e]\,, \tag{8}$$

where $m \in \{0, \ldots, M - 1\}$, $e \in \{0, \ldots, N - 1\}$ and $\psi_k[i, e]$ denotes the basis expansion coefficients for subcarrier e. The

Slepian sequences $\boldsymbol{u}_i \in \mathbb{R}^M$ with elements $u_i[m]$ are defined as the eigenvectors of the matrix $\boldsymbol{C} \in \mathbb{R}^{M\times M}$ with elements

$$[\boldsymbol{C}]_{i,\ell} = \frac{\sin\left[2\pi(i-\ell)\nu_{\mathrm{Dmax}}\right]}{\pi(i-\ell)} \tag{9}$$

where $i,\ell = 0,1,\ldots,M-1$, i.e. $\boldsymbol{C}\boldsymbol{u}_i = \lambda_i \boldsymbol{u}_i$. The approximate dimension of the time-concentrated and bandlimited signal space is $D \geq \lceil 2\nu_{\mathrm{Dmax}} M \rceil + 1$ [2, Sec. 3.3], which means that the eigenvalues λ_i rapidly decay to zero for $i > D$. For a detailed analysis of the estimation error please refer to [4].

Inserting the basis expansion (8) into (7) gives

$$y[m,e] \approx \sum_{k=1}^{K}\sum_{i=0}^{D-1} u_i[m]\psi_k[i,e]d_k[m,e] + v[m,e]\,. \tag{10}$$

We can obtain a linear MMSE estimate of the subcarrier coefficients $\hat{\psi}_k[i,e]$ jointly for all K users but individually for every subcarrier e as described in [11], [12].

After $\hat{\psi}_k[i,e]$ are evaluated for all $e \in \{0,\ldots,N-1\}$, an estimate for the time-variant frequency response is given by $\hat{g}'_k[m,e] = \sum_{i=0}^{D-1} u_i[m]\hat{\psi}_k[i,e]$. Additional noise suppression is obtained if we exploit the correlation between the subcarriers. This correlation is present since the essential support of the channel impulse response is smaller than the number of subcarriers. We compare the Fourier based approach with a new Slepian subspace based method in the next section

IV. Subspace Projection in the Frequency Domain

A. Sample-Spaced Delay Tap-Line Model: Fourier Subspace

In the case of a sample-spaced delay tap-line model a simple partial discrete Fourier transform is sufficient [6] in order to exploit the correlation between the individual subcarriers,

$$\hat{g}_k[m,e] = \boldsymbol{f}^{\mathrm{T}}[e]\sum_{e'=0}^{N-1}\boldsymbol{f}[e']\hat{g}'_k[m,e']. \tag{11}$$

where

$$\boldsymbol{f}[e] = \begin{bmatrix} \mathrm{e}^{-\mathrm{j}2\pi e/N} \\ \vdots \\ \mathrm{e}^{-\mathrm{j}2\pi(L-1)e/N} \end{bmatrix} \in \mathbb{C}^L\,. \tag{12}$$

The projection operation in (11) exploits the fact, that the impulse response has maximum length L while in the frequency domain N subcarrier coefficients are estimated. Due to this projection a noise reduction by L/N can be achieved.

However, the path delays in realistic channels are real valued. In this case the projection (11) leads to biased results. We will show this by an analytic analysis of the square bias in Section V. In order to reduce the square bias we apply a dual version of the concepts presented in Section III.

B. Non-Sample-Spaced Delay Tap-Line Model: Slepian Subspace

We can write (3) in the frequency domain as

$$g(t,f) = \sum_{r=1}^{R}\alpha_r(t)\mathrm{e}^{-\mathrm{j}2\pi\tau_r(t)f} \tag{13}$$

for $f \in \mathbb{R}$ omitting the dependence on k.

In an OFDM system the channel (13) is sampled in the frequency domain using N subcarriers $g[m,e]$, $e \in \{0,\ldots,N-1\}$ with spacing $1/(T_{\mathrm{C}}N)$ resulting in

$$g[m,\tilde{e}] = \sum_{r=1}^{R}\alpha_r(mT_{\mathrm{C}})\mathrm{e}^{-\mathrm{j}2\pi\theta_r[m]\tilde{e}} \tag{14}$$

for $\tilde{e} \in \{-N/2,\ldots,N/2-1\}$ and N even. The normalized path delay $\theta_r[m] = \frac{\tau_r(mT_{\mathrm{C}})}{T_{\mathrm{C}}N}$ fulfills $0 \leq \theta_r[m] < L_{\mathrm{ess}}/N < 1$. We note that due to the DFT $e = ((\tilde{e}+N) \mod N)$. L_{ess} is the essential support of the physical channel impulse response (3). Due to the band-limiting filter at the transmitter and the receiver side the overall impulse response is enlarged and its support $L > L_{\mathrm{ess}}$

For m fixed, the sequences $g[m,\tilde{e}]$ (14) span a subspace that has dual properties to the Slepian subspace in the time-domain (see Section III). The frequency index $\tilde{e}$ is dual to the time index m and the delay parameter θ_r is dual to the Doppler shift ν_r.

The path delays θ_r are from the interval $[0,\theta_{\max}]$ where $\theta_{\max} = \max(\theta_r)$. The snapshot length is N. Thus, the corresponding subspace has dimension $D' \geqslant \lceil \theta_{\max} N \rceil + 1$.

The DPS sequences $\tilde{\boldsymbol{u}}'_i \in \mathbb{C}^N$ with elements $\tilde{u}'[e]$ are the eigenvectors of matrix $\boldsymbol{C'}$ with elements

$$[\boldsymbol{C'}]_{i,\ell} = \frac{\sin\left[2\pi(i-\ell)\theta_{\max}/2\right]}{\pi(i-\ell)} \tag{15}$$

where $i,\ell = 0,1,\ldots,N-1$. The subspace for noise reduction is spanned by the shifted DPS sequences

$$u'_i[e] = \tilde{u}'_i[e]\mathrm{e}^{-\mathrm{j}2\pi\theta_{\max}e/2}\,. \tag{16}$$

The shifting of the DPS sequences in (16) is done to take into account the non-symmetric interval $\theta \in [0,\theta_{\max}]$ of the time delays. It can be verified that $\boldsymbol{u}'_i$ are the eigenvectors of the covariance matrix of a uniform power delay profile $\boldsymbol{R}_{gg}$ given by [8, Appendix A].

$$[\boldsymbol{R}_{gg}]_{i,\ell} = \frac{1-\mathrm{e}^{2\pi\mathrm{j}\theta_{\max}(i-\ell)}}{2\pi\mathrm{j}\theta_{\max}(i-\ell)}\,. \tag{17}$$

We define

$$\boldsymbol{f}^{(\mathrm{S})}[e] = \begin{bmatrix} u'_0[(e+N/2) \mod N] \\ \vdots \\ u'_{D'-1}[(e+N/2) \mod N] \end{bmatrix} \in \mathbb{C}^{D'}\,. \tag{18}$$

for $e \in \{0,\ldots,N-1\}$ and N even. Inserting $\boldsymbol{f}^{(\mathrm{S})}[e]$ in (11) we perform a frequency domain Slepian subspace projection that achieves a noise variance reduction by D'/N. Then, the channel estimates $\hat{\boldsymbol{g}}_k[m]$ are inserted into (5) to enable data detection.

The Slepian subspace projection in the time domain is dual to the one in the frequency domain. In the time domain the Doppler frequencies are from the interval $\nu \in [-\nu_{\mathrm{Dmax}},\nu_{\mathrm{Dmax}}]$ and the observation window in time has length M. In the frequency domain the time delays of the individual paths are in the range $\theta \in [0,\theta_{\max}]$ and the observation window in frequency has length N.

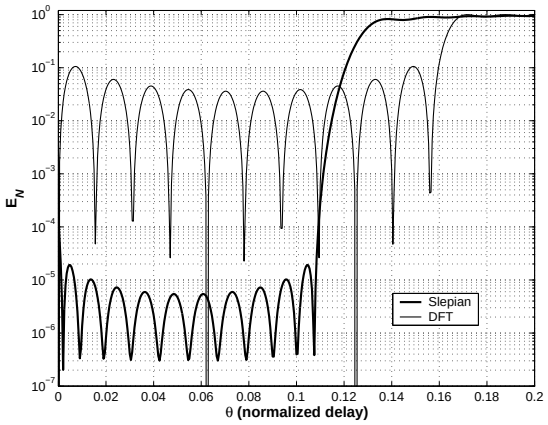

Fig. 2. Mean error characteristic E_N versus normalized delay θ. For $N = 64$ subcarriers, essential support of the impulse response $L_{\mathrm{ess}} = 8$, maximum normalized delay $\theta_{\max} = 0.125$ and $D' = 11$ dimensions we compare the shifted DPS sequences (denoted 'Slepian') with the Fourier basis functions (denoted 'DFT') with $L = 11$ dimensions.

V. Square Bias of Frequency Domain Subspace Projection

Square bias results for the time domain subspace projection are provided in [4]. We will give results for the frequency domain case in this section.

We define the instantaneous error characteristic

$$E(e,\theta) = \Big|1 - \boldsymbol{f}^{\mathrm{T}}[(e+N/2) \mod N] \cdot \cdot \sum_{\ell=0}^{N-1} \boldsymbol{f}^{*}[\ell] \mathrm{e}^{-\mathrm{j}2\pi\theta((e-\ell+N/2) \mod N)}\Big|^2 . \quad (19)$$

for $e \in \{0,\ldots,N-1\}$ and $0 \le \theta \le \theta_{\max}$. Furthermore, we define the power delay profile $\eta^2(\theta) = \mathbb{E}\{|h(t,\theta N T_{\mathrm{C}})|^2\}$ and express the square bias per subcarrier as

$$\mathrm{bias}^2[e] = \int_0^1 E(e,\theta)\eta^2(\theta)\mathrm{d}\,\theta. \quad (20)$$

The square bias for all subcarriers that is due to the frequency domain Slepian subspace projection is finally given by

$$\mathrm{bias}_N^2 \triangleq \frac{1}{N}\sum_{q=0}^{N-1}\mathrm{bias}^2[e] = \int_0^1 E_N(\theta)\eta^2(\theta)\mathrm{d}\,\theta\,, \quad (21)$$

where the mean error characteristic is defined as

$$E_N(\theta) = \frac{1}{N}\sum_{e=0}^{N-1} E(e,\theta)\,. \quad (22)$$

Figure 2 plots $E_N(\theta)$ for $N = 64$ subcarriers, essential support of the impulse response $L_{\mathrm{ess}} = 8$, maximum normalized delay $\theta_{\max} = L_{\mathrm{ess}}/N = 0.125$ and $D' = 11$ dimensions of the subspace. Using Fig. 2 we can easily see, that for a power delay profile $\eta^2(\theta)$ with a maximum delay below $\theta_{\max}$ the square bias (21) will be several magnitudes smaller than the one of the Fourier based approach which uses $L = 11$ basis functions as well

VI. Simulation of the COST 259 GSCM Channel Model

In our implementation of the COST 259 model, the GSCM [13], one or several mobile stations (MS) are placed within the simulation area. The region covers a set of base stations (BS) each having several antennas. A velocity vector is assigned to each MS and near scatterers are placed around the MS. In addition to the scatterers round the MS far scatterers are placed within the simulation area. Such additional scatterers are important for achieving higher delay spreads. The scatterers are grouped into clusters. For each cluster an angular delay power spectra (ADPS) is defined. A cluster may encompass an area of several hundred meters in a macro cellular environment. Specular reflection at the scatterers is assumed and a ray tracing tool calculates the impulse responses by summing up all possible paths according to (3). A path starts at the transmitter and is bounced at one or two scatterers before hitting the receiver. The length of the path is used to calculate the delay. A more detailed description on the implementation of the model is given in [7].

In contrast to many other channel models the COST 259 channel model does not use a quantized tap-delay line structure, where paths occur exactly within one delay bin only. The delays in our model vary over time due to the movement of the users and the changing lengths of the traced paths. This effect causes problems to simple receive algorithms which assume quantized delays of paths. Assuming quantized delays does not reflect reality and may result in optimistically-biased performance of the receive algorithm.

To include this effect, sampling at chip rate is not sufficient. In our case we use a four times oversampled input signal for the channel model. This signal is filtered using a root raised cosine filter. Inside the channel model an even higher sample rate is used. At the output of the model the four times oversampled signal is again root raised cosine filtered and down converted to the chip rate of the receiver.

We have chosen the generalized typical urban (GTU) environment for all simulations using the GSCM. This is one of the four specified macro cellular environments of COST 259. All mobiles are uniformly spread within the cell area.

The COST 259 channel model includes large-scale and short-scale effects. The first ones are modeled stochastically, the short scale fading is implicitly given by the superposition of the arriving paths. For the focus of this paper the large scale effects are not taken into account since we assume perfect power control for slow changes of the channel. Thus only short scale effects are visible to the receiver.

We assume that all impinging user signals are received at the same time. This is achieved by subtracting the smallest delay from all paths of a user.

VII. System Parameters

The system operates at carrier frequency $f_{\mathrm{C}} = 2\,\mathrm{GHz}$ and the $K = 32$ users move with velocity $v = 70\,\mathrm{km/h}$. This gives a Doppler bandwidth of $B_{\mathrm{D}} = 133\,\mathrm{Hz}$ corresponding to $\nu_{\mathrm{D}} = 0.0027$. The number of subcarriers is $N = 64$ and the length of

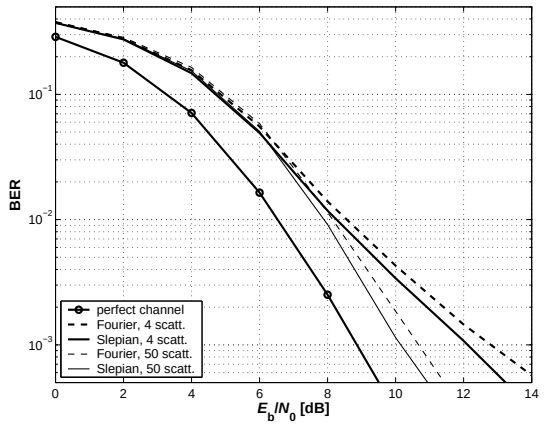

Fig. 3. BER versus E_b/N_0 for the multi-user MC-CDMA uplink after 4 iterations with $K = 32$ users moving at $v = 70\,\mathrm{km/h}$. The Slepian subspace in the time domain has dimension $D = 3$ and in the frequency domain $D' = 11$ (denoted 'Slepian'). The result for the partial Fourier transform with dimension $L = 11$ is denoted 'Fourier'. For comparison the performance with perfect channel knowledge is shown too.

the OFDM symbol with cyclic prefix is $P = G+N = 79$. The data block consists of $M = 256$ OFDM symbols with $J = 60$ OFDM pilot symbols. The system is designed for a maximum velocity $v_\mathrm{max} = 100\,\mathrm{km/h}$ which results in $D = 3$ for the Slepian basis expansion. All simulation results are averaged over 100 independently generated data blocks. We assume a maximum normalized path delay of $\theta_\mathrm{max} = 0.125$ $(L_\mathrm{ess} = 8)$ and use $D' = 11$ shifted DPS sequences for noise suppression in the frequency domain. For comparison we use $L = D' = 11$ Fourier basis functions.

For data transmission, a convolutional, non-systematic, non-recursive, 4 state, rate $R_C = 1/2$ code with generator polynomial $(5, 7)_8$ is used.

We use two different scenarios; one with 50 scatterers in order to model rich scattering and one with 4 scatterers for a low diversity situation. In both cases the scatterers are randomly distributed in a region with a radius of $200\,\mathrm{m}$ around the mobile station.

VIII. Results

In Fig. 3, we illustrate the multi-user MC-CDMA uplink performance in terms of bit error rate (BER) versus E_b/N_0 with iterative time-variant channel estimation based on the Slepian subspace projection after 4 iterations.

We apply the Slepian basis expansion in the time-domain in order to estimate each time-variant subcarrier individually [4]. Then, we use a second subspace projection in the frequency domain exploiting the correlation of the individual subcarriers. For this second projection in the frequency domain we compare the receiver performance for the Slepian subspace projection (18) (denoted 'Slepian') and the partial Fourier transform (12) (denoted 'Fourier'). The reduced square bias of the Slepian subspace (see Fig. 2) leads to a BER performance that is 1 dB better at a BER of 10^{-3} compared to the Fourier based method. With increasing diversity the performance gain reduces slightly.

In [4] we studied the gain of the Slepian subspace projection over the Fourier basis expansion in the time-domain. In the time-domain the gain is more pronounced than the gain in the frequency domain (that can be additionally obtained after a Slepian subspace projection in the time domain).

IX. Conclusions

Simulation results show that an iterative receiver using the Slepian subspace projection in the time and frequency domain for time-variant channel estimation is able to deal with the realistic GSCM in a multi-user system. Only two channel parameters, an upper bound on the Doppler shift and an upper bound on the support of the impulse response are needed for the design of the basis function. The Slepian subspace projection in the frequency domain is most beneficial for scenarios with small delay spread and few scatterers.

Acknowledgements

We would like to thank Christoph F. Mecklenbräuker for helpful comments and suggestions.

References

[1] H. Atarashi, S. Abeta, and M. Sawahashi, "Broadband packet wireless access appropriate for high-speed and high-capacity throughput," in *IEEE Vehicular Technology Conference (VTC)*, vol. 1, May 2001, pp. 566–570.

[2] D. Slepian, "Prolate spheroidal wave functions, Fourier analysis, and uncertainty - V: The discrete case," *The Bell System Technical Journal*, vol. 57, no. 5, pp. 1371–1430, May-June 1978.

[3] T. Zemen and C. F. Mecklenbräuker, "Time-variant channel equalization via discrete prolate spheroidal sequences," in *37th Asilomar Conference on Signals, Systems and Computers*, Pacific Grove (CA), USA, November 2003, pp. 1288–1292, invited.

[4] ——, "Time-variant channel estimation using discrete prolate spheroidal sequences," *IEEE Trans. Signal Processing*, accepted for publication.

[5] A. M. Sayeed, A. Sendonaris, and B. Aazhang, "Multiuser detection in fast-fading multipath environment," *IEEE J. Select. Areas Commun.*, vol. 16, no. 9, pp. 1691–1701, December 1998.

[6] D. Schafhuber, G. Matz, and F. Hlawatsch, "Adaptive Wiener filters for time-varying channel estimation in wireless OFDM systems," in *IEEE International Conference on Acoustics, Speech, and Signal Processing (ICASSP)*, vol. 4, April 2003, pp. 688–691.

[7] H. Hofstetter and G. Steinböck, "A geometry based stochastic channel model for MIMO systems," in *ITG Workshop on Smart Antennas*, Munich, Germany, January 2004.

[8] O. Edfors, M. Sandell, J.-J. van de Beek, S. K. Wilson, and P. O. Börjesson, "OFDM channel estimation by singular value decomposition," *IEEE Trans. Commun.*, vol. 46, no. 7, pp. 931–939, July 1998.

[9] J. Du and Y. G. Li, "D-BLAST OFDM with channel estimation," *EURASIP Journal on Applied Signal Processing*, vol. 5, pp. 605–612, 2004.

[10] Y. G. Li and L. J. Cimini, "Bounds on the interchannel interference of OFDM in time-varying impairments," *IEEE Trans. Commun.*, vol. 49, no. 3, pp. 401–404, March 2001.

[11] T. Zemen, "OFDM multi-user communication over time-variant channels," Ph.D. dissertation, Vienna University of Technology, Vienna, Austria, July 2004.

[12] T. Zemen, C. F. Mecklenbräuker, J. Wehinger, and R. R. Müller, "Iterative joint time-variant channel estimation and multi-user decoding for MC-CDMA," *IEEE Trans. Wireless Commun.*, revised.

[13] J. Fuhl, A. Molisch, and E. Bonek, "Unified channel model for mobile radio systems with smart antennas," *IEE Proceedings on Radar, Sonar and Navigation*, vol. 145, no. 1, pp. 32–41, Feb. 1998.